

Does ADS 9346 have a low-mass companion?

Olga V. Kiyaveva, Maxim Yu. Khovritchev, Agrippina M. Kulikova, Natalya V. Narizhnaya, Tatyana A. Vasilyeva and Arina A. Apetyan

Central Astronomical Observatory, Russian Academy of Sciences, 65/1 Pulkovskoye Chaussee, St. Petersburg, 196140, Russia; deimos@gaoran.ru

Received 2021 July 15; accepted 2021 August 17

Abstract Based on the photographic and CCD observations of the relative motion of the A and B components of the binary system ADS 9346 obtained with the 26-inch refractor of Pulkovo Observatory during 1979–2019, we discover an invisible companion associated with star A. Comparison of the ephemerides with the positional and spectroscopic observations allowed us to calculate the preliminary orbit of the photocenter ($P = 15$ yr). The minimal mass of the companion is approximately $0.13 M_{\odot}$. The existence of the invisible low-mass companion is implied by the IR-excess based on IRAS data. To confirm this, additional observations of the radial velocity near the periastron need to be carried out.

Key words: (stars:) binaries: visual — stars: low-mass — stars: individual (ADS 9346)

1 INTRODUCTION

We have to take binary and multiple systems into account when we study the formation of stars and exoplanets and the further dynamical evolution of stellar groups and systems of exoplanets. This fact is reflected in many works on this topic (i.e., [Reipurth et al. 2014](#)). That is why the search for multiple stars is a relevant observational problem, especially in the context of studies on exoplanet systems (i.e., [Mugrauer 2019](#)). The search for binary and multiple stars is a traditional topic for Pulkovo Observatory (i.e., [Grosheva 2006](#)). We present the results of a study on the visual binary star ADS 9346 (WDS 14410+5757, HD 129580, HIP 71782), which has been a part of the 26-inch Pulkovo refractor observational program since 1979.

This paper continues the series of studies on ADS 9346 ([Kiyaveva et al. 2008, 2010](#)). In the first work, based on all observations from the Washington Double Star (WDS) catalog, the radius of curvature of the observed arc and the dynamical mass of the binary star with an elliptical orbit were calculated. The value of the dynamical mass ($4.2 \pm 1.6 M_{\odot}$) is significantly different from what is expected according to the photometric data ($\approx 2.2 M_{\odot}$). In the second work, applying the apparent motion parameters (AMP) method, we obtained three possible orbits with small inclination with respect to the plane of projection and orbital periods ≈ 2000 yr. However, to achieve agreement with the expected mass, we had to increase the parallax from Hipparcos (18.9 ± 0.9 mas, ESA 1997)

up to 24 mas. Also, based on the Pulkovo photographic (1979–2005) and CCD (2003–2007) observations, the perturbation in separation between the components was discovered with the assertion that the system might have another companion with an orbital period of 4 yr (or a multiple of 4).

Nowadays, new data have become available: the series of Pulkovo CCD observations have been extended for 12 yr; the parallaxes from Gaia Data Release 2 (DR2) ([Gaia Collaboration et al. 2018](#)) (17.8573 ± 0.0318 mas for star A and 17.8652 ± 0.0384 mas for star B) and Gaia Early Data Release 3 (EDR3) ([Gaia Collaboration et al. 2021](#)) (17.8383 ± 0.0161 mas for star A and 17.8720 ± 0.0429 mas for star B) are even smaller than parallaxes published in Hipparcos. Therefore, we have to take another look at our previous results.

In this work, we study the discovered perturbations in the relative motion and define the preliminary inner orbit of the possible companion.

2 OBSERVATIONAL DATA ANALYSIS

Our study is based on CCD observations (77 series) obtained with the 26-inch refractor of the Pulkovo Observatory during 2003–2019 ([Izmailov et al. 2010, 2020](#)), which are available online in the Pulkovo database¹ and the Strasbourg astronomical Data Center (CDS)².

¹ <http://izmccd.puldb.ru/vds.htm>

² <https://cdsarc.unistra.fr/viz-bin/cat/J/AN/341/762>

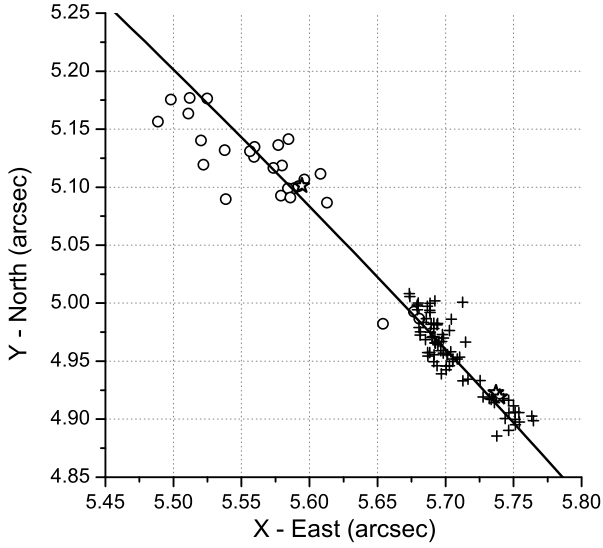


Fig. 1 Observations obtained with the 26-inch refractor during 1979–2019: *open circles* – photographic, *crosses* – CCD, *open stars* – Hipparcos, Gaia DR2 and EDR3, *solid line* – the ephemeris of the orbit of the wide pair.

The photographic observation data from 1979 to 2005 (36 plates, 11 average annual positions) obtained with the same telescope was supplemented by CCD observation results and as a first approximation reflect the orbital motion of the wide pair at this section of the orbit (Kiselev et al. 2014). In the framework of this study, we attempted to remeasure astronegatives which is described in Section 3. The series of Pulkovo observations from 1979 to 2019 is presented in Figure 1.

The results of 102 observations from 1830 to 2015 are presented in the WDS catalog (Mason et al. 2016). The first observation by John Herschel is very different from the following measurements, so we will rely on the observation by Wilhelm Struve, obtained in 1830, as the first observation. Besides, we omit one observation from 1908 as it is an obvious mistake. We use observations from WDS to define the orbit of the wide pair obtained more accurately with the AMP method.

The Gaia DR2 catalog (Gaia Collaboration et al. 2018) contains observations of the radial velocity only for star A. According to CDS, the spectroscopic observations of the radial velocities for ADS 9346 are not presented in published works. However, there is one high-precision observation of star A obtained with the Hobby-Eberly telescope in 2006 (Deka-Szymankiewicz et al. 2018). There are no observations of the radial velocity of component B in those works. The only long-term series of observations of both components is published in Kiyeva et al. (2010). The velocities were measured in 2000–2008 with CORAVEL – a correlation radial velocity spectrometer constructed by A. Tokovinin (Tokovinin

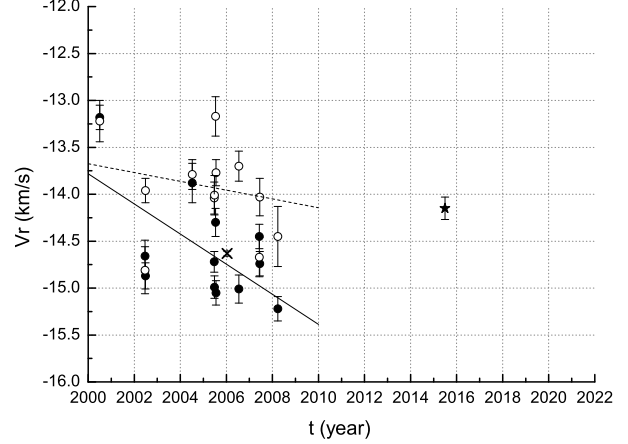


Fig. 2 The radial velocity observations of the components: *filled circles* – star A velocity, *open circles* – star B velocity, *times sign* – Hobby-Eberly observation, *a star* – Gaia observation. *Lines* show the linear trends for star A (*solid line*) and star B (*dashes*).

1987), mounted on the 1-m telescope of Crimean Astrophysical Observatory. An assumption was made that according to the Tokovinin criteria (Tokovinin 1988) star A might have a companion. Figure 2 depicts the results of those measurements and their dependency over time. Lines represent linear trends corresponding to the radial accelerations for each component on a given interval. The observations cannot reflect the orbital motion of the external pair because the acceleration of the more massive component $\dot{V}_{r,A} = -0.160 \pm 0.060 \text{ km s}^{-1} \text{ yr}^{-1}$ is greater than $\dot{V}_{r,B} = -0.047 \pm 0.061 \text{ km s}^{-1} \text{ yr}^{-1}$. This fact confirms the possibility of star A having an additional long-period companion.

Gaia DR2 contains the parallaxes of both components with the same accuracy (0.03 mas). In Gaia EDR3, the error of the parallax is 0.016 mas for star A and 0.043 mas for star B. The parallax of component B is measured with a lower accuracy and there are no observations of the radial velocity.

The fact that in Gaia EDR3 the parallax of star A is measured with a higher accuracy suggests that the orbital period of the possible companion should be significantly larger than the observational period of Gaia, the orbit should have a larger eccentricity and during observations the companion should be located near apoastron.

3 ASTRONEGATIVE REMEASUREMENTS

As already mentioned in the Introduction, the appearance of new high-precision data motivated us to conduct this research: more dense series of Pulkovo CCD observations, Gaia observations and radial velocity measurements. The methodology of astronegative measurements has also improved in the recent decade. That is why it seems

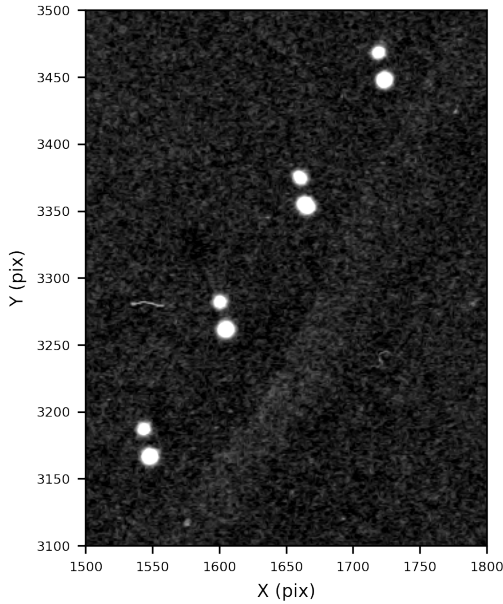


Fig. 3 Images of the visual binary ADS 9346 at the fragment of plate 10356 obtained with the 26-inch refractor of Pulkovo Observatory on 1979 May 13.

reasonable to take advantage of new resources and repeat the digitization of astronegatives and the analysis of scans to improve the accuracy of the photographic series for ADS 9346. The main goal of the procedure is to make sure that quasi-periodic perturbation that takes place for the CCD series is also present in old observations and is not a systematic effect only associated with the CCD series.

Previously, we employed a flatbed scanner to digitize the photographic plates with the images of ADS 9346. The main disadvantage of this scanner is the unstable field of systematic errors from one scanning to another (and even during the process of digitization). In the past few years, the MDD measuring complex has been actively used at Pulkovo Observatory (for detailed information see [Izmailov et al. 2016](#); [Khovritchev et al. 2021](#)).

Figures 3 and 4 display the fragment of the photographic plate with the images of the ADS 9346 components and the structure of those images. This gives us a common understanding of the quality of astronegatives. All measurements were made utilizing the technique described in [Khovritchev et al. \(2021\)](#). To define the orientation and scale, we relied on reference stars such that positions at the epoch of observations were taken from the Gaia EDR3 catalog. In total we analyzed 37 astronegatives. The reference stars with the necessary signal to noise ratio were present in 27 of those astronegatives. Only these plates were analyzed later on. There were from 10 to 22 exposures taken on each plate, therefore we were able to estimate the intrinsic accuracy of the measurements: for $\rho - 7$ mas and for $\theta - 0.05$ deg.

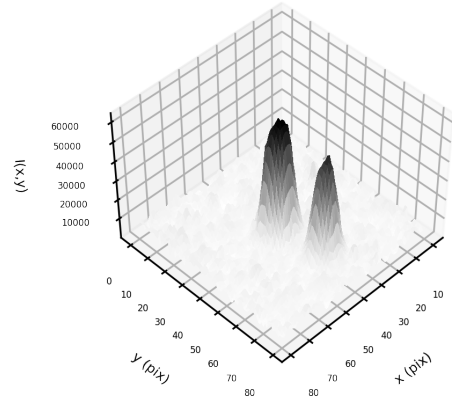


Fig. 4 The image structure of ADS 9346 on plate 10356.

These estimates correspond to the level of accuracy of $1.5 \mu\text{m}$ which is in agreement with data from [Khovritchev et al. \(2021\)](#).

Figure 1 plots the relative motion in the system ADS 9346. The initial series of photographic observations is systematically inconsistent with the series of CCD observations of ρ . It is difficult to come up with the reason for such divergence. The photographic series were obtained with the filter ZhS-18. The response curves of the photographic emulsion and the CCD sensor differ significantly. This could lead to a shift due to atmospheric dispersion, since the color indexes of the components are very different. Therefore, for the purposes of our research, the correction to the photographic series was determined empirically. The CCD series are shifted by 30 mas for ρ , which corresponds to $1 - \sigma$ for the photographic series. The series for $\rho(t)$ are characterized by noticeable quasi-periodic perturbations. They are more evident in CCD observations and can be noticed at a similar range in the photographic data. This allows us to assume that the attempt to repeat the digitization process was successful. The existence of variations greater than the standard error of ρ suggests that this can be associated with the invisible low-mass companion in the system ADS 9346. More strictly it can be demonstrated applying Fourier analysis to the CCD series and the sum of the photographic and the CCD series. Figure 5 illustrates the power spectrums. As can be seen, using all observations we can obtain the period estimate close to 20 yr. We should note that these series are quite irregular, therefore later this estimate will be improved in a more natural way for a given task.

4 PHOTOMETRIC-BASED COMPONENT MASSES

The a priori mass estimate is one of the requirements of the AMP method. The high-precision photometric

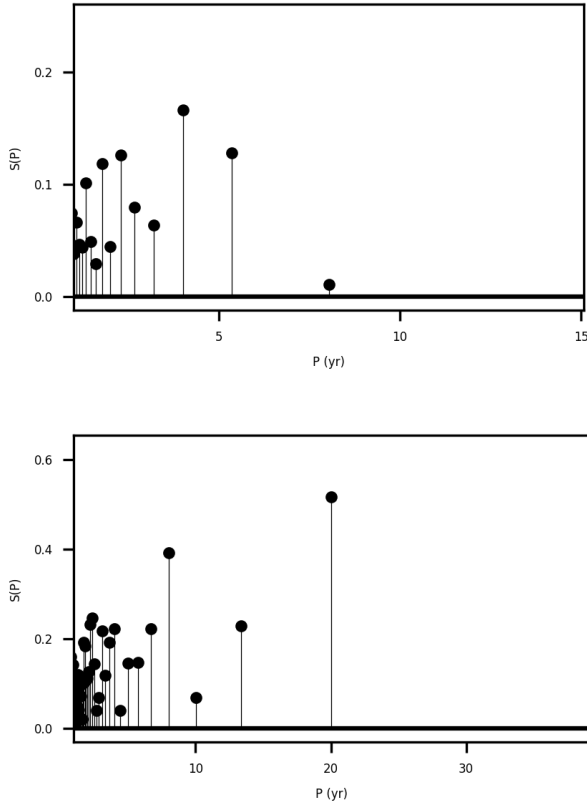


Fig. 5 Power spectrums for the series of $\rho(t)$. The top plot takes into account only CCD observations while the bottom plot features the whole series (photographic observations plus CCD observations).

data allow us to hope for a sufficient accuracy in the mass determination. Taking into account the trigonometric parallax and the apparent magnitude estimates from Gaia EDR3 along with the metallicity and the interstellar extinction data, we can easily locate the components of ADS 9346 on the color-magnitude diagram. The PARSEC³ (Bressan et al. 2012) tool makes it possible to plot the necessary isochrones (see Fig. 6). Then, we can interpolate and choose the isochrones and the points on those isochrones for the best fit in relation to the positions of components A and B on the diagram.

As a result of the spectral analysis during the radial velocity determination for star A (Deka-Szymankiewicz et al. 2018), the values of the key parameters for this component were obtained; for instance, the metallicity $[\text{Fe}/\text{H}] = 0.22$ and the apparent color index $(B - V) = 0.9$ mag. The spectrum gives the intrinsic color index $(B - V)_0 = 0.86$ mag, meaning that the interstellar reddening $E(B - V) = 0.04$ mag. Thus, we can easily estimate the interstellar extinction and reddening for the Gaia EDR3 bands utilizing the data from Wang & Chen (2019). The

³ <http://stev.oapd.inaf.it>

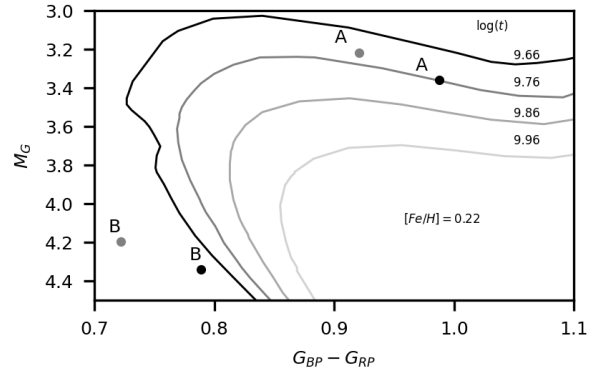


Fig. 6 PARSEC-isochrones in the vicinity of ADS 9346 on the color-magnitude diagram corresponding to different ages and the metallicity $[\text{Fe}/\text{H}] = 0.22$ (taking the interstellar extinction and reddening into account). *Black circles* mark the positions of the components according to the interstellar extinction from the works Deka-Szymankiewicz et al. (2018); Wang & Chen (2019). *Grey circles* signify the positions according to the Gaia DR2 data.

obtained values are the following: $A_G = 0.105$ mag and $E(G_{BP} - G_{RP}) = 0.055$ mag. On the other hand, there are direct measurements of the interstellar extinction and reddening in Gaia DR2 (Gaia Collaboration et al. 2018): $A_G = 0.249$ mag and $E(G_{BP} - G_{RP}) = 0.123$ mag. The formal standard errors for these values do not exceed 0.01 mag.

The results of the mass and age determinations for star A are presented in Deka-Szymankiewicz et al. (2018): $m_A = 1.08 M_\odot$ and $\log(t) = 9.96$. These values were obtained following a technique similar to the one described in the first paragraph of this section. However, the authors based their research on the trigonometric parallaxes from Hipparcos-2 (van Leeuwen 2007): $p_t = 18.03 \pm 0.69$ mas. They suggest that the estimated value $p_t = 22.2 \pm 4.23$ mas corresponds to the spectral data, which is not in agreement with the weighted average from Gaia EDR3 ($p_t = 17.86 \pm 0.04$ mas) within the limits of 1σ . We suppose that the independent measurements from Hipparcos-2 and Gaia are trustworthy, meaning that the mass determination needs to be reconsidered. The credibility of the results becomes debatable due to the uncertainties in the interstellar extinction and reddening estimates mentioned above (see Fig. 6). Middle ground can be found in mass estimates of about $1.21 \pm 0.1 M_\odot$ for star A and $1.05 \pm 0.15 M_\odot$ for star B.

Thus, the analysis of the photometric and spectral data gives us $2.26 M_\odot$ for the total mass and $\log(t) = 9.76$ for age, which obviously corresponds better to high metallicity. The age determination in Deka-Szymankiewicz et al. (2018) seems too ambitious. A star that is older than

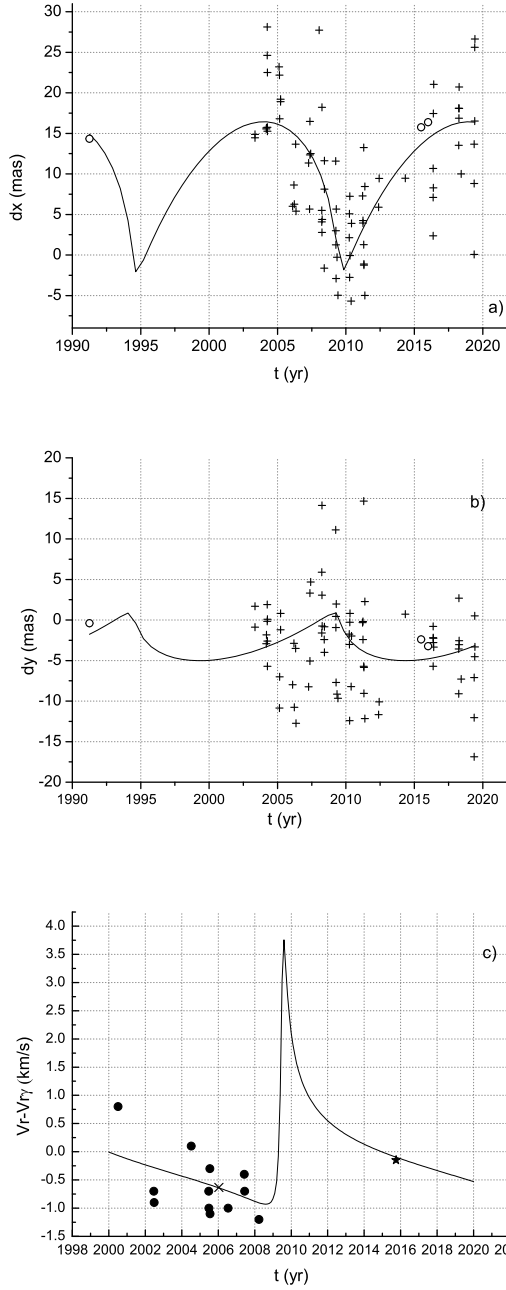


Fig. 7 A comparison between the ephemerides and the positional observations of the companion in right ascension (a), declination (b) and observed radial velocity (c). For the positional observations: *crosses* – CCD observations, *open circles* – Gaia and Hipparcos. For the radial velocity observations: *filled circles* – CORAVEL, *times signs* – Hobby-Eberly observations, *a star* – Gaia DR2.

9 Gyr with metallicity $[Fe/H] = 0.22$ is less likely to be located in the solar neighborhood than a star with the same metallicity and an age that is a little over 5.7 Gyr.

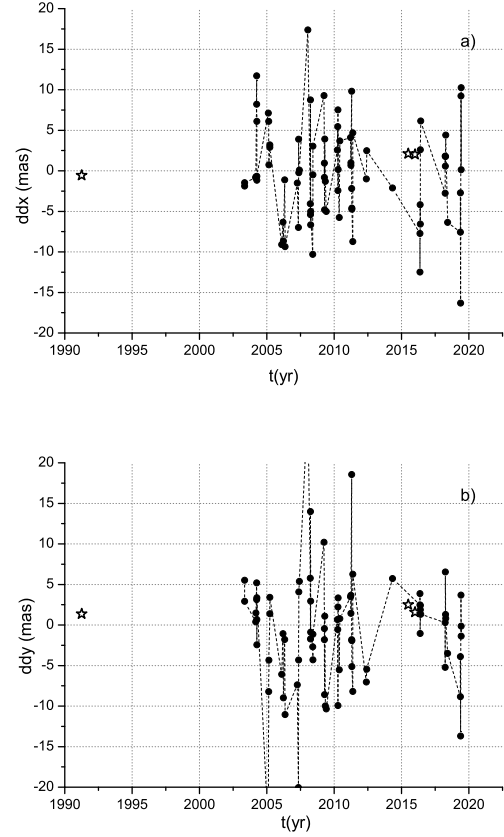


Fig. 8 The residuals (after taking into account the companion) of right ascension (a) and declination (b). *Filled circles* – CCD observations, *open circles* – the Hipparcos and Gaia data.

5 CALCULATION OF THE ORBITAL PARAMETERS OF THE PHOTOCENTER OF STAR A PLUS THE INVISIBLE LOW-MASS COMPANION

The observational results obtained with the 26-inch refractor of Pulkovo Observatory during 1979–2019 are presented in Figure 1. As mentioned above, there is a perturbation in the relative motion with a period around 20 yr. To get more reliable orbital period estimates for the possible invisible companion, we added the Hipparcos and Gaia DR2 data at epoch 2015.5 and Gaia EDR3 data at epoch 2016.0. The weights for observations were calculated according to the standard measurement errors.

We cannot determine which star has a companion using the relative positions, but the fact that star A is more massive, which also has a larger acceleration than star B, gives us a reason to assume that only star A can have the long-period companion. Moreover, the list of stars with possible low-mass companions from the work [Kervella](#)

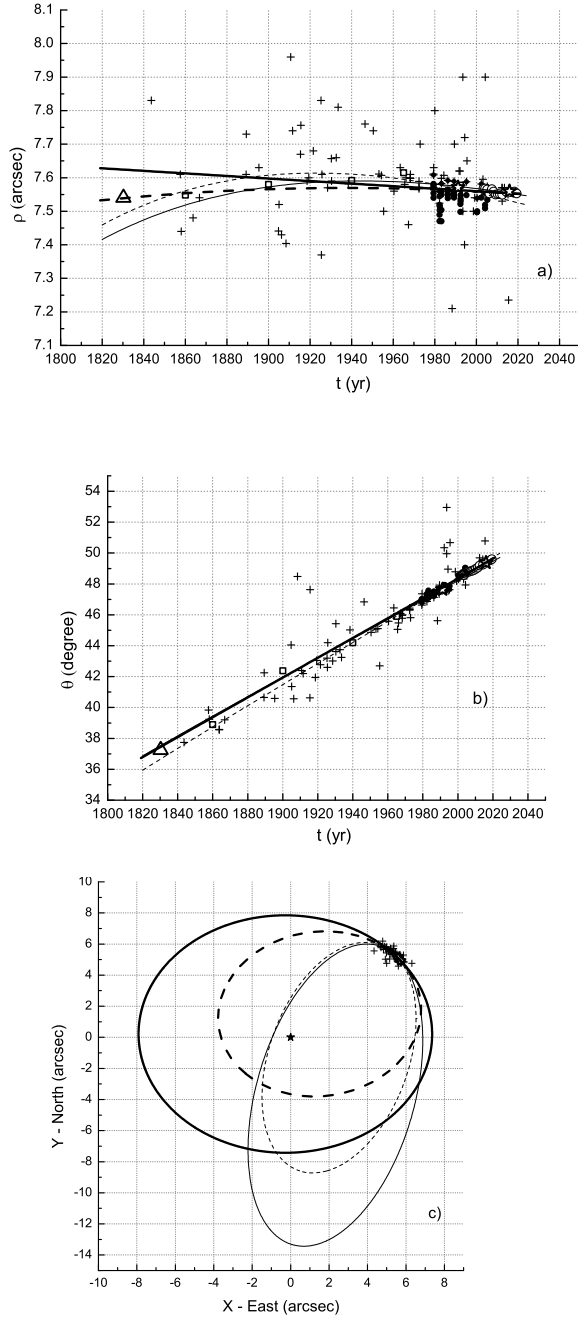


Fig. 9 The comparison between the orbits of the external pair A-B and observations. *Crosses* – WDS observations, *open squares* – the reference series, *filled* and *open circles* – the Pulkovo photographic and CCD observations, *a triangle* – the first observation by Struve, *stars* – the Hipparcos and Gaia EDR3 observations, *bold solid line* – the orbit with $2.4 M_{\odot}$ (var. 2), *bold dashes* – the orbit with $4.1 M_{\odot}$, *thin solid line* – the orbit from Izmailov (2019) with weights, *thin dashes* – that without weights.

et al. (2019) contains star A, which is another confirmation of the existence of the companion.

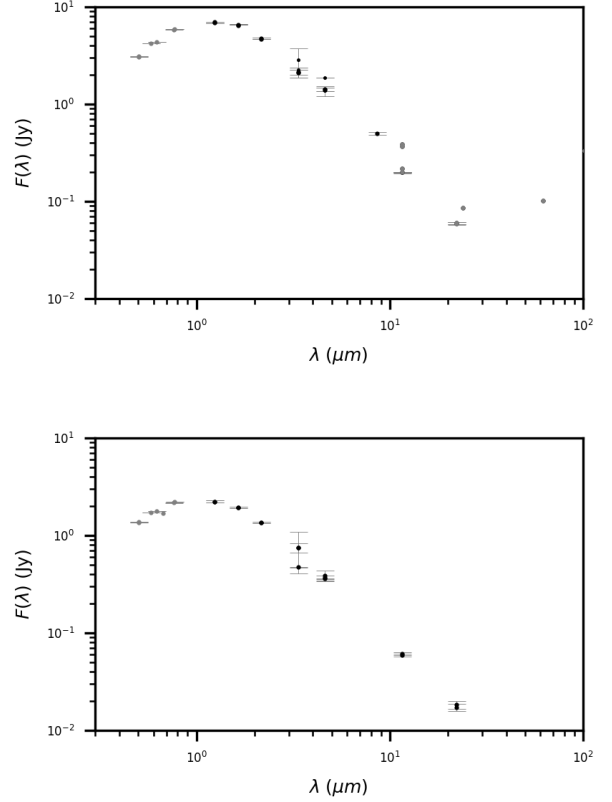


Fig. 10 SED for the components of ADS 9346 (top – for star A, bottom – for star B). The data are from Gaia DR2, Gaia EDR3, 2MASS, WISE and IRAS.

The relative motion of the binary star with one companion can be expressed with the following equations:

$$x_i = x_0 + \dot{x}(t_i - t_0) + \ddot{x}(t_i - t_0)^2/2 + BX_i + GY_i, \quad (1)$$

$$y_i = y_0 + \dot{y}(t_i - t_0) + \ddot{y}(t_i - t_0)^2/2 + AX_i + FY_i. \quad (2)$$

Here $x_i = \rho \sin \theta$, $y_i = \rho \cos \theta$ — the apparent coordinates in the tangential plane, $X_i = \cos E_i - e$, $Y_i = \sqrt{1 - e^2} \sin E_i$ — the orbital coordinates calculated considering the orbital period P , the periastron epoch T and the eccentricity e for each companion. A , B , F and G are the unknown Thiele-Innes elements which define the geometrical elements of the Kepler orbit of the photocenter a_{ph}, i, ω and Ω . The unknown parameters $x_0, \dot{x}, \ddot{x}, y_0, \dot{y}$ and \ddot{y} reflect the relative motion of the center of mass of star B in relation to the center of mass of the system star A plus the invisible companion. Utilizing these parameters, we can calculate the AMP and the orbit of the external pair.

First of all, we considered periods in the range from 10 to 15 yr with a step size of 1 yr, because the series of CCD observations is 16 yr long. T and e were obtained using the

brute-force search method with a step size of 0.1 yr for T and 0.1 for e . The stopping criterion of the method is the minimal standard deviation $\sigma_{xy} = \sqrt{\sigma_x^2 + \sigma_y^2}$. Here $\sigma_x = \sqrt{\sum p_i(dx_i)^2/n}$ and p_i are the weights corresponding to the observational error, and σ_y is calculated in the same way.

According to the given criterion, all orbits with periods from 11 to 15 yr fit the observational data equally well. Solving Equations (1) and (2), we can obtain the Thiele-Innes elements (that define the orbit of the companion) with great confidence. Hence, we use independent observations of the radial velocities as criteria: $t = 2006.03$, $\Delta V_{rA} = V_{rA} - V_{rA\gamma} = -0.632 \pm 0.027 \text{ km s}^{-1}$ (Deka-Szymankiewicz et al. 2018) and $t = 2015.5$, $\Delta V_{rA} = -0.15 \pm 0.12 \text{ km s}^{-1}$ (Gaia DR2), if we set $V_{rA\gamma} \approx -14.0 \text{ km s}^{-1}$ (see Fig. 7).

Additionally, we compare the trend obtained using the ephemerides from 2000–2008 with the observed radial velocity acceleration of star A ($-0.16 \pm 0.06 \text{ km s}^{-1} \text{ yr}^{-1}$).

We get the best solution (an agreement within the confidence intervals) for the orbit with $P = 15 \pm 0.5 \text{ yr}$, $e = 0.86 \pm 0.01$ and $T = 2009.5 \pm 0.1$. The corresponding ephemerides: $t = 2006.0$, $\Delta V_{rA} = -0.637 \text{ km s}^{-1}$; $t = 2015.5$, $\Delta V_{rA} = -0.07 \text{ km s}^{-1}$; $\dot{V}_{rA} = -0.11 \text{ km s}^{-1} \text{ yr}^{-1}$.

The solution of Equations (1) and (2), as well as the radial velocity semi-amplitude of the visible component, the semi-major axis of the relative orbit and the elements of the Kepler orbit corresponding to the Thiele-Innes elements, is presented in Table 1.

If we believe that the photocenter coincides with the visible component, we can calculate the minimal mass of the companion m_s which depends on the parallax and the mass of the visible component M_1 . Here we use the weighted average parallax of star A from Gaia EDR3: $p_t = 17.838 \pm 0.016 \text{ mas}$.

The residual errors of the Kepler orbital elements were obtained with the Monte Carlo method in the following way. All residuals were randomly altered 50 times with the dispersion 9 mas which corresponds to the variations (see Table 1). We calculated the mean solution shifted in relation to the initial (model) solution. The errors were calculated in relation to the model solution. The shift and errors in the mean solution are presented in brackets.

The graphical representation of the observations and the ephemerides of right ascension (dx), declination (dy) and radial velocity (ΔV_r) are shown in Figure 7.

There is a systematic difference between space observations and observations with the 26-inch refractor which is significant for some stars. For this star, the difference between the Gaia DR2 system and the CCD observations is 6 mas for ρ . Therefore, it is worth

Table 1 The Parameters of the Relative Motion of the Photocenter of star A plus Low-mass Companion at 2010.0

| | |
|------------------------------|-------------------------------|
| P_{in} (yr) | 15 ± 0.5 |
| x_0 (mas) | 5695.1 ± 1.3 |
| y_0 (mas) | 4960.3 ± 1.5 |
| \dot{x} (mas yr $^{-1}$) | 5.07 ± 0.14 |
| \dot{y} (mas yr $^{-1}$) | -6.63 ± 0.17 |
| \ddot{x} (mas yr $^{-2}$) | -0.1130 ± 0.0302 |
| \ddot{y} (mas yr $^{-2}$) | 0.0968 ± 0.0345 |
| T (yr) | 2009.5 ± 0.1 |
| e | 0.86 ± 0.01 |
| B (mas) | -8.33 ± 1.30 |
| A (mas) | 2.39 ± 1.51 |
| G (mas) | -7.97 ± 1.72 |
| F (mas) | -3.41 ± 2.01 |
| a_{ph} (mas) | $11.55(-0.23) \pm 2.46(2.45)$ |
| i ($^\circ$) | $110.8(-15.8) \pm 22.0(14.3)$ |
| ω ($^\circ$) | $314.7(+17.5) \pm 32.1(28.6)$ |
| Ω ($^\circ$) | $266.1(+7.5) \pm 21.1(19.9)$ |
| a (a.e.) | 7.0 |
| K_{ph} (km s $^{-1}$) | 2.4 |
| M_1 (M_\odot) | 1.21 |
| m_s (M_\odot) | 0.129 |
| σ_x (mas) | 9.20 |
| σ_y (mas) | 9.39 |
| σ_{xy} (mas) | 13.14 |

The Kepler elements correspond to the Thiele-Innes elements. The shifts in the mean solution and its error are in brackets. a_{ph} – the semi-major axis of the photocentric orbit, a – the semi-major axis of the relative orbit, K_{ph} – the half range of the photocentric radial velocity. The minimal mass of the companion m_s is calculated considering the parallax from Gaia EDR3 and the mass of the visible component (M_1).

mentioning that in the $dx(t)$ plot the changes in the Gaia DR2 (2015.5) and the Gaia EDR3 positions are in full agreement with the ephemerides for this area.

We can conclude that the effect is significant ($a \approx 11 \text{ mas}$), the inclination of the orbit is close to 90° and in the tangential plane the companion moves in the line of the orbital node ($\Omega \approx 270^\circ$), which is in agreement with the $dx(t)$ plot. There is still an unaccounted effect with a possible period of 4 yr at the $dy(t)$ plot.

Figure 8 displays the residuals after taking into account the companion with the orbital period of 15 yr.

The calculated orbit with the period of 15 yr can be improved or changed when the radial velocity observations in the area of periastron become available.

6 ESTIMATION OF THE VALUES OF ORBITAL ELEMENTS FOR THE A-B PAIR

One of the the best ways to determine the initial orbit of a visual binary using a short arc in the framework of the two-body problem is the AMP method. It was described numerous times starting from 1980 (i.e., Kiselev & Kiyaveva 1980; Kiyaveva & Romanenko 2020). After taking the motion of the companion into account (see Table 1) we calculated the AMP at $t_0 = 2010.0$ (the

Table 2 The Parameters of the Relative Motion of the A-B Pair, Calculated for Different Conditions

| Var. | t_0 | ρ (") | θ (°) | μ ("/yr) | ψ (°) | β_1 (°) | M_{A+B} (M_\odot) | S_1 (") | β_2 (°) | S_2 (") |
|------|--------|------------------------|-----------------|------------------|--------------|---------------|-------------------------|-----------|---------------|-----------|
| 1 | 2010.0 | 7.5524 ± 0.0014 | 48.945 0.010 | 0.0083 0.0002 | 142.6 1.0 | 0 10 | 4.4 | 0.175 | 0 6 | 0.524 |
| 2 | 2010.0 | 7.5560 ± 0.0008 | 48.989 0.004 | 0.0085 0.0001 | 141.5 1.3 | ± 14 7 | 4.1 | 0.098 | 0 10 | 0.381 |

Two solutions are shown: 1 – using the CCD observations with the companion ($P_{in} = 15$ yr); 2 – using the CCD observations without the companion. The best fit corresponds to the minimum of S_1 , if the mass M_{A+B} is undefined, or S_2 , if $M_{A+B} = 2.4 M_\odot$.

Table 3 The Orbital Parameters of the A-B Pair

| Ref | This work solution 1 | | This work solution 2 | | Izmailov (2019) | | Kiyeva et al. (2010) |
|-------------------------|----------------------|-------------|----------------------|-------------|-----------------|---------------|----------------------|
| P (yr) | 5435 ± 519 | 2455 213 | 5725 556 | 2749 220 | 2547 1031 | 4130 2230 | 2644 2239 |
| T (yr) | 3612 ± 128 | 3165 103 | 3170 599 | 3323 814 | 1528 398 | 1526 954 | 3100 2241 |
| e | 0.07 ± 0.02 | 0.45 .04 | 0.05 .04 | 0.39 .04 | 0.75 .20 | 0.80 .18 | 0.34 .22 |
| a (") | 7.38 ± 0.47 | 5.24 .30 | 7.64 .49 | 5.56 .30 | 11.48 5.20 | 15.57 7.72 | 5.78 2.39 |
| i (°) | 0 ± 17 | 0 20 | 0 16 | 14 8 | 71 11 | 74 11 | 19 8 |
| $\Omega + \omega$ (°) | 162 ± 128 | 224 86 | 127 126 | 225 - | - - | - - | 212 22 |
| Ω (°) | - \pm | - - | - - | 142 43 | 16 38 | 18 61 | 159 - |
| ω (°) | - \pm | - - | - - | 83 36 | 273 18 | 283 20 | 53 - |
| M_{A+B} (M_\odot) | 2.4 | 4.2 | 2.4 | 4.1 | 41 | 38 | 4.8 |
| σ_ρ (mas) | 113.5 | 112.4 | 112.8 | 112.3 | 114.0 | 112.6 | 122.2 |
| σ_τ (mas) | 131.2 | 131.1 | 130.5 | 130.4 | 131.8 | 132.4 | 132.4 |

For orbits determined in this paper, $\Delta V_r = 0 \text{ km s}^{-1}$ is fixed. Total masses for all orbits correspond to the parallaxes from Gaia EDR3 (17.8425 mas). ω and Ω can differ by 180° . Due to small inclinations of orbits in relation to the tangential plane, in 2010 we could obtain only $\omega + \Omega$. Now, utilizing the Gaia data, we can separate these parameters.

separation between the components (ρ) in arcseconds, the positional angle (θ) in degrees, the apparent relative motion (μ) in mas per year and the positional angle of the apparent motion (ψ) in degrees) and their errors using the following simple expressions:

$$\rho = \sqrt{x^2 + y^2}, \quad \theta = \arctan \frac{x}{y},$$

$$\mu = \sqrt{\dot{x}^2 + \dot{y}^2}, \quad \psi = \arctan \frac{\dot{x}}{\dot{y}}.$$

$$\varepsilon_\rho = \sqrt{(x\varepsilon_x)^2 + (y\varepsilon_y)^2} / \rho,$$

$$\varepsilon_\theta = \sqrt{(y\varepsilon_x)^2 + (x\varepsilon_y)^2} / \rho^2,$$

$$\varepsilon_\mu = \sqrt{(\dot{x}\varepsilon_{\dot{x}})^2 + (\dot{y}\varepsilon_{\dot{y}})^2} / \mu,$$

$$\varepsilon_\psi = \sqrt{(\dot{y}\varepsilon_{\dot{x}})^2 + (\dot{x}\varepsilon_{\dot{y}})^2} / \mu^2.$$

In addition, we also obtain from the observation the parallax, the relative radial velocity and the total mass of the system.

We use the weighted average of the parallax p_t from Gaia EDR3, which is 17.842 ± 0.046 mas.

We set $V_{rA\gamma} = -14 \text{ km s}^{-1}$. Then, according to the radial velocity observations during 2000–2008, the relative radial velocity $V_{rB} - V_{rA} \approx 0 \pm 0.5 \text{ km s}^{-1}$. For a star with an orbital period of about several thousand years, this value will not change significantly in 10 yr.

The radius of curvature ρ_c can be calculated utilizing the following equation

$$\rho_c = \left| \frac{(\dot{x}^2 + \dot{y}^2)^{1.5}}{\dot{x}\ddot{y} - \dot{y}\ddot{x}} \right|. \quad (3)$$

However, the determination of ρ_c with Equation (3) is associated with uncertainties due to large errors \ddot{x} and \ddot{y} ($\rho_c = 2.2'' \pm 4.0''$), and as a result we cannot determine the distance between the components r at the moment t_0 using Equation (4)

$$r^3 = 4\pi^2(M_A + M_B) \frac{\rho \rho_c}{\mu^2} |\sin(\psi - \theta)|. \quad (4)$$

That is why for all variations we get the set of elliptical orbits which satisfy the following condition

$$\frac{\rho}{p_t} \leq r \leq \frac{8\pi^2}{v^2}(M_A + M_B). \quad (5)$$

Here v is the space velocity of star B with respect to star A.

From this set of orbits we choose the best fit for all observations of the binary star from its discovery. This solution is measured by the angle

$$\beta = \pm \arccos \frac{\rho}{p_t r}$$

between the direction to the companion and its projection on the tangential plane, as was suggested in [Kiselev & Romanenko \(1996\)](#).

The total mass of all visible components and the companion equals $2.26 M_\odot$. Taking into account the influence of the possible companion, we suppose that the total mass of the system is unknown. Then we correct the value using all available observations. When choosing the best fit, we do not compare the observations directly, but rely on agreement between the Thiele-Innes elements (A, B, F, G) instead. They can be calculated using the geometrical orbital elements (a, i, ω, Ω) without observations, and also using the dynamical elements (P, T, e) combined with observations separated in time ([Kiyaveva 1983](#)). The criterion for this method is the minimum of the function

$$S = \sqrt{\Delta A^2 + \Delta B^2 + \Delta F^2 + \Delta G^2}. \quad (6)$$

Here $\Delta A, \Delta B, \Delta F$ and ΔG are the differences between the Thiele-Innes elements obtained in two ways. As opposed to the direct comparison between the observations and the ephemerides, in this case we do not need to assign weights to particular heterogeneous observations which inevitably introduce some subjectivity. However, it is important to have several reliable points spaced along the entire arc near the middle of the observational sector.

As the range of observations from the WDS catalog is too wide, we calculated the additional reference series through the middle of the observational sector. All observations before 1991 (Hipparcos) were split in 30–40 yr intervals and the AMP (ρ, θ) were calculated for the mean moment of each interval. Besides, the reference series includes the first observation conducted by Struve, as well as Hipparcos and Gaia data, and the AMP obtained using the photographic Pulkovo observations. Comparing the AMP-orbits with the reference series, we get the best formal solution.

The results — AMP, β_1 and the total mass M_{A+B} , which correspond to the minimum of S_1, β_2 and S_2 with

fixed mass $M_{A+B} = 2.4 M_\odot$ — are presented in [Table 2](#). Two solutions are shown: the AMP obtained relying on [Equations \(1\) and \(2\)](#) (see [Table 1](#)) taking into account the companion with a period of 15 yr (solution 1) and homogeneous CCD observations without the companion (solution 2).

We obtained the orbital elements for both variants with the expected total mass $2.4 M_\odot$ and the mass corresponding to the minimum of function S . The results are presented in [Table 3](#).

For comparison we also display the orbits from [Izmailov \(2019\)](#) with a period of 2547 yr (without weights) and 4130 yr (with weights), as well as the orbit obtained in the work [Kiyaveva et al. \(2010\)](#) utilizing the homogeneous photographic observations, AMP at the epoch 1990.0, for which the obtained total mass was also too high. Total masses for all orbits correspond to the parallaxes from Gaia EDR3. Within the limits of errors we achieve a good agreement of all three AMP-orbits with the mass that exceeds $4 M_\odot$.

The errors of the AMP-orbits are defined by the errors of the initial data. The errors of the elements obtained in 2010 are too large due to the large parallax error used back then.

Since $\Delta V_r \approx 0.0 \text{ km s}^{-1}$, the location of the node can be determined to 180° . Since β is small, we can conclude that the plane of the inner orbit is oriented near the tangential plane. A small inclination is characteristic for all AMP-orbits. With the expected mass of $2.4 M_\odot$, we get almost circular orbits in the tangential plane.

Since the length of a series of observations is longer than the orbital periods of a possible companion, the effect of its action is blurred and does not affect the calculation of the AMP. Taking our preliminary orbit into account does not improve the agreement with observations, but it does not distort the result either. The new orbits obtained in this work do not contradict the previous studies. [Figure 9](#) presents observations and ephemerides of radically different orbits.

7 DISCUSSION

The question of the presence of the low-mass companion can be finally resolved by only using additional observations. Let us consider all the currently known arguments confirming the presence or absence of the low-mass companion.

1. Signs of a companion for star A were obtained utilizing positional data but are in agreement with independent radial velocity observations as well.
2. In Gaia EDR3, there is a parameter that characterizes the quality of astrometric observations, as well as their agreement with models of the linear movement

of the photocenter of a star, PSF and other effects. This parameter is `astrometric_excess_noise_sig` or D as in the original paper [Lindegren et al. \(2012\)](#). A significant excess of residual variance over the sum of squared errors of individual effects ($D > 2$) might be caused by different reasons or their combination. For instance, the images of bright stars are often overexposed. Another reason for increasing the value D is the difference between the real movement of stars and a linear (5-parameter) model. In case of ADS 9346, $D = 12.7$ for star A and $D = 142.8$ for star B. An impact that a companion might have on total brightness with separation less than $0.2''$ is likely insignificant. Therefore, the reason why the parameter D is large for the ADS 9346 components might be associated with the overexposure, as the majority of stars surrounding ADS 9346 with magnitudes in the range from 7^m to 8.5^m are characterized by the parameter D of the same order. Thus, we can conclude that the additional Gaia EDR3 data limit the mass of a possible companion by $0.5 M_{\odot}$. Otherwise, the parameter D would be larger (the difference in magnitudes between star A and its companion would be 5^m).

3. Another argument confirming that star A has a companion follows from the analysis of the spectral energy distribution (SED) based on the photometric observations conducted during the implementation of different observational programs in different spectral ranges from Gaia to IRAS (Gaia DR2, Gaia EDR3, 2MASS ([Skrutskie et al. 2006](#)), WISE ([Wright et al. 2010](#)) and IRAS ([Abrahamyan et al. 2015](#))). The SED for the components of ADS 9346 are presented in [Figure 10](#). As can be seen from the figure, there is an infrared (IR)-excess for star A at $100 \mu m$ (obtained by IRAS). According to [Trilling et al. \(2007\)](#), this can be considered an indication of duplicity. This emission is generated by dust clouds near a relatively old star. The analysis performed by Trilling and coauthors ([Trilling et al. 2007](#)) affirms that stable large-scale dust structures near stars like the A-component of ADS 9346 can exist in regions of stable resonances in case of stellar multiplicity.

8 CONCLUSIONS

The main result of our study is the confirmation of perturbation in the relative motion of A-B components of ADS 9346 based on observations conducted with the 26-inch Pulkovo refractor. The observed variations can be explained by the existence of a low-mass ($0.129 M_{\odot}$) companion that revolves around star A with a period of 15 yr. The orbit of the companion is highly eccentric, and the passage of the periastron in 2009 coincided with active

observations with the 26-inch refractor, but there were no radial velocity observations that could confirm or disprove our conclusion. We calculated the preliminary orbit of the photocenter of star A plus the invisible companion consistent with the available radial velocity observations.

The presence of a companion is indirectly confirmed by the IR-excess in the emission of star A. For stars more than 5 Gyr old, dust radiation at a wavelength of $100 \mu m$ can be caused by dust structures confined in regions of stable resonances.

Following the AMP method, we calculated new orbits of the external pair with a total mass given according to estimates based on photometric data and a mass obtained in best agreement with astrometric observations.

There are two possible reasons why these mass estimates differ:

- The accuracy of astrometric observations collected over 200 yr is low. The orbit that is in agreement with all observations can correspond to any mass (see [Table 3](#) and [Figure 7](#)). The Thiele-Innes elements cannot be strictly determined on short arcs, therefore the formal best solution ($4.1 M_{\odot}$) is one of the possible solutions. However, it does contradict other data. That is why we give two solutions: with the formally obtained mass and the expected mass.
- There is still a possibility that component B has another short-period companion which we cannot detect according to our observations. Indirect evidence of such a scenario is that while there is a radial velocity measurement for component A in Gaia, there is none for component B; the parallax error of component B in Gaia EDR3 is 3 times greater than that of component A; as can be seen from [Figure 6](#), component B strongly moves away from the isochrone to the blue side. All this gives reason to believe that the properties of this star do not fit into the formal model.

The AMP method allows the consistent use of the object observation results obtained by different methods, and therefore leads to more reliable results, which is confirmed by a comparison with the orbits published in [Izmailov \(2019\)](#). For high-volume determination of orbits for the purpose of statistical studies, formal methods are acceptable, but on short arcs they cannot lead to a reliable result. For the study of individual stars, the AMP method is preferable, supplemented by agreement with all available photometric data and radial velocity measurements.

Acknowledgements The reported study was funded by RFBR according to the research projects 19-02-00843 A and 20-02-00563 A and with partial support of the grant 075-15-2020-780 from the Government of the Russian Federation and the Ministry of Higher Education and Science.

This work has made use of data from the European Space Agency (ESA) mission *Gaia* (<https://www.cosmos.esa.int/gaia>), processed by the *Gaia* Data Processing and Analysis Consortium (DPAC, <https://www.cosmos.esa.int/web/gaia/dpac/consortium>). Funding for the DPAC has been provided by national institutions, in particular the institutions participating in the *Gaia* Multilateral Agreement.

References

- Abrahamyan, H. V., Mickaelian, A. M., & Knyazyan, A. V. 2015, *Astronomy and Computing*, 10, 99
- Bressan, A., Marigo, P., Girardi, L., et al. 2012, *MNRAS*, 427, 127
- Deka-Szymankiewicz, B., Niedzielski, A., Adamczyk, M., et al. 2018, *A&A*, 615, A31
- Gaia Collaboration, Brown, A. G. A., Vallenari, A., et al. 2018, *A&A*, 616, A1
- Gaia Collaboration, Brown, A. G. A., Vallenari, A., et al. 2021, *A&A*, 649, A1
- Grosheva, E. A. 2006, *Astrophysics*, 49, 397
- Izmailov, I., Rublevsky, A., & Apetyan, A. 2020, *Astronomische Nachrichten*, 341, 762
- Izmailov, I. S. 2019, *Astronomy Letters*, 45, 30
- Izmailov, I. S., Khovricheva, M. L., Khovrichev, M. Y., et al. 2010, *Astronomy Letters*, 36, 349
- Izmailov, I. S., Roshchina, E. A., Kiselev, A. A., et al. 2016, *Astronomy Letters*, 42, 41
- Kervella, P., Arenou, F., Mignard, F., & Thévenin, F. 2019, *A&A*, 623, A72
- Khovritchev, M. Y., Robert, V., Narizhnaya, N. V., et al. 2021, *A&A*, 645, A76
- Kiselev, A. A., & Kiyaveva, O. V. 1980, *AZh*, 57, 1227
- Kiselev, A. A., & Romanenko, L. G. 1996, *Astronomy Reports*, 40, 795
- Kiselev, A. A., Kiyaveva, O. V., Izmailov, I. S., et al. 2014, *Astronomy Reports*, 58, 78
- Kiyaveva, O. V. 1983, *AZh*, 60, 1208
- Kiyaveva, O. V., Gorynya, N. A., & Izmailov, I. S. 2010, *Astronomy Letters*, 36, 204
- Kiyaveva, O. V., Kiselev, A. A., & Izmailov, I. S. 2008, *Astronomy Letters*, 34, 405
- Kiyaveva, O. V., & Romanenko, L. G. 2020, *Astronomy Letters*, 46, 555
- Lindegren, L., Lammers, U., Hobbs, D., et al. 2012, *A&A*, 538, A78
- Mason, B. D., Wycoff, G. L., Hartkopf, W. I., Douglass, G. G., & Worley, C. E. 2016, *VizieR Online Data Catalog*, B/wds
- Mugrauer, M. 2019, *MNRAS*, 490, 5088
- Reipurth, B., Clarke, C. J., Boss, A. P., et al. 2014, in *Protostars and Planets VI*, eds. H. Beuther et al., 267
- Skrutskie, M. F., Cutri, R. M., Stiening, R., et al. 2006, *AJ*, 131, 1163
- Tokovinin, A. A. 1987, *Soviet Ast.*, 31, 98
- Tokovinin, A. A. 1988, *Astrophysics*, 28, 173
- Trilling, D. E., Stansberry, J. A., Stapelfeldt, K. R., et al. 2007, *ApJ*, 658, 1289
- van Leeuwen, F. 2007, *A&A*, 474, 653
- Wang, S., & Chen, X. 2019, *ApJ*, 877, 116
- Wright, E. L., Eisenhardt, P. R. M., Mainzer, A. K., et al. 2010, *AJ*, 140, 1868